Available online at www.sciencedirect.com
ScienceDirect
Vision Research 46 (2006) 3845–3852
Vision Research
www.elsevier.com/locate/visres

An unusual X-linked retinoschisis phenotype and biochemical characterization of the W112C *RS1* mutation

Alessandro Iannaccone [a,*], Marco Mura [a,1], Frank M. Dyka [b], Maria Laura Ciccarelli [c], Beverly M. Yashar [d,e], Radha Ayyagari [e], Monica M. Jablonski [a], Robert S. Molday [b]

[a] *Hamilton Eye Institute, Department of Ophthalmology, University of Tennessee Health Science Center, 930 Madison Avenue, Suite 731, Memphis, TN 38163, USA*
[b] *Centre for Macular Research, Department of Biochemistry and Molecular Biology, University of British Columbia, Vancouver, BC, Canada*
[c] *Division of Ophthalmology, Fatebenefratelli Hospital-AFaR, Isola Tiberina, Rome, Italy*
[d] *Department of Human Genetics, University of Michigan, Ann Arbor, MI, USA*
[e] *Department of Ophthalmology and Visual Sciences, University of Michigan, Ann Arbor, MI, USA*

Received 14 April 2006; received in revised form 2 June 2006

Abstract

A 52-year-old subject harboring an *RS1* gene W112C mutation presented with a prominent and asymmetric tapetal-like retinal sheen. Transient ERG responses were smaller and slower in the eye with the more extensive sheen, an association that, to our knowledge, had not been previously reported. An ON-pathway dysfunction explained the abnormalities of the transient but not those of the flicker ERGs. Although in vitro studies showed that the W112C mutant retinoschisin is present only in the cellular fraction and is not secreted, disease expression was remarkably mild, consistent with the notion of the existence of genetic and/or epigenetic disease modifiers.

Keywords: Retinoschisis; Tapetal-like reflex; Genetics; Electroretinogram (ERG); Bipolar cell

1. Introduction

X-linked recessive juvenile retinoschisis (XLRS) is a hereditary retinal disease characterized by splitting of the neuroretina, resulting from mutations in the *RS1* gene (Sauer et al., 1997). Over the past few years, the cellular localization and molecular characterization of the 224-amino acid protein encoded by *RS1*, retinoschisin, has been partially elucidated, suggesting a role in retinal cell adhesion (Molday, Hicks, Sauer, Weber, & Molday, 2001; Reid, Yamashita, & Farber, 2003; Weber et al., 2002; Wu & Molday, 2003), and revealing an important role in synaptic transmission at the bipolar cell level (Molday et al., 2001; Takada et al., 2004), thereby providing important insights into the clinical, functional, and pathologic features of XLRS. In its most typical clinical manifestations, XLRS is characterized by foveal stellate cystic changes, causing reduced visual acuity in childhood, and peripheral retinoschisis (Falcone & Brockhurst, 1993; George, Yates, & Moore, 1995, 1996; Kellner, Brummer, Foerster, & Wessing, 1990). Among the less common manifestations is a tapetal-like, silver to golden patchy reflex, which has been reported in up to 38% of cases (George, Yates, & Moore, 1996). Although it has been hypothesized that this reflex may be due to excess extracellular K^+ ions, either resulting from excessive release from activated retinal neurons or from impaired Müller cell K^+ reuptake (de Jong, Zrenner, van Meel, Keunen, & van Norren, 1991), its true biological significance remains unknown.

Here, we report the case of a man with unusually late-onset and mild visual symptoms associated with a distinctive

* Corresponding author. Fax: +1 901 448 5028.
E-mail address: iannacca@utmem.edu (A. Iannaccone).
[1] Present address: Department of Ophthalmology, Academic Medical Center, University of Amsterdam, The Netherlands.

0042-6989/$ - see front matter © 2006 Elsevier Ltd. All rights reserved.
doi:10.1016/j.visres.2006.06.011

retinal clinical phenotype, mainly characterized by the aforementioned prominent retinal tapetal-like metallic reflexes, accompanied by functional manifestations at the ERG level that paralleled the extent of the sheen, and in whom a *RS1* mutation was identified, offering also the opportunity for biochemical in vitro characterization of the mutant protein.

2. Methods

All studies reported herein conformed to the Declaration of Helsinki and study protocols were approved by the Institutional Review Boards of the participating institutions.

2.1. Clinical exam

Family history was collected from the proband at the time of examination, along with a standard questionnaire for patients with hereditary retinal diseases. Visual acuity was measured by means of conventional Snellen charts in a clinical setting. Undilated and dilated anterior segment exam and posterior segment exam were conducted by slit lamp biomicroscopy. Scleral depression under indirect ophthalmoscopy was applied for further evaluation of the retinal far periphery. Digital color photographs of the fundus and an intravenous fluorescein angiogram were obtained according to standard methodologies following maximal pharmacological pupil dilation.

2.2. ERG testing protocol

Full-field ERG testing was performed in a clinical setting to ascertain the functional retinal status of this patient according to a previously reported protocol (Koenekoop et al., 2002; Pannarale et al., 1996). Tests were conducted on a day distinct from that of the clinical exam. In brief, after 30 min of full dark-adaptation and maximal pharmacological pupil dilation, dark-adapted rod-driven responses were recorded with a −2.25log candela [cd] s/m^2, 0.5 Hz white strobe flash, followed by maximal (mixed rod-cone) dark-adapted (0.5 Hz) and photopic (1 Hz transient and 30 Hz flicker) light-adapted (steady background of approximately 30 cd/m^2) ERG responses, recorded with a flash of 0.18log cd s/m^2. Monopolar contact lens electrodes applied under dim red light following topical anesthesia were used to measure the responses. Reference and ground electrodes were applied on the forehead midline and one earlobe, respectively.

2.3. Mutation screening

After obtaining from the proband informed consent to molecular genetic testing for further work-up, whole blood was collected in EDTA-containing tubes and shipped to the University of Michigan, where genomic DNA was extracted, and all the six exons of the *RS1* gene were PCR amplified and subsequently sequenced as previously described (Retinoschisis Consortium, 1998).

2.4. Retinoschisin mutants

The human RS1 cDNA was subcloned as described earlier (Wu & Molday, 2003) into pCEP4 vector (Invitrogen) using the *Xho*I and *Hin*dIII restriction sites. To introduce the W112C mutation the quick change site-directed mutagenesis kit (Stratagene) was used. The constructs were sequenced to verify the desired mutation and the absence of random mutations. The RS1 3R10 mAb (Weber et al., 2002) was purified and coupled to CNBr-activated Sepharose 2B as previously described (Molday, Cook, Kaupp, & Molday, 1990).

2.5. Cell culture and transfection

EBNA 293 cells (American Type Culture Collection) were transfected in 10 cm dishes with 20 μg of plasmid DNA per dish, containing wildtype RS1 or the W112C mutation, using the calcium phosphate transfection procedure as previously described (Wu & Molday, 2003). Briefly, 500 μl of BBS-buffered saline (50 mM *N*,*N*-bis(2-hydroxyethyl)-2-aminoethane, 280 mM NaCl, 1.4 mM Na_2PO_4, pH 6.95) was added drop-wise to a DNA solution containing 250 mM calcium chloride and incubated for 20 min at room temperature. DNA was then added to exponentially growing EBNA 293 cells and incubated at 37 °C under 5% CO_2. The DNA containing medium was replaced with regular medium the next day and the cells and cell culture supernatant were harvested two days later.

2.6. Protein analysis

Protein extraction, gel electrophoresis and Western blotting were performed essentially as previously described (Wang et al., 2002, 2006; Wu & Molday, 2003; Wu, Wong, Kast, & Molday, 2005). Briefly, the cellular fraction was obtained by washing the cells twice in PBS (137 mM NaCl, 2.7 mM KCl, 10 mM Na_2HPO_4, 1.8 mM KH_2PO_4) by low speed centrifugation. The final pellet was re-suspended in 200 μl of PBS containing 20 mM *N*-ethylmaleimide (NEM). Cells were lysed by adding 400 μl of PBS containing 20 mM NEM, 2% Triton X-100 and complete protease inhibitor (Roche Applied Science). After 1 h at 4 °C the solution was centrifuged at 100,000 *g* for 10 min and the supernatant was retained for gel electrophoresis. The secreted fraction was obtained by centrifuging the supernatant at 15,000 rpm in a Sorvall SS 34 rotor for 20 min to remove debris. The supernatant was then incubated for 2 h with an immunoaffinity resin consisting of the RS1 3R10 antibody coupled to Sepharose 2B (Wu & Molday, 2003). After washing several times with column buffer (20 mM Tris–HCl, 0.2% Triton X-100, 20 mM NEM), bound RS1 was eluted with 200 μl of 4% SDS in column buffer.

Twenty microlitres of each eluted and cellular fraction was used for SDS gel electrophoresis and Western blotting. Proteins were denatured in an SDS cocktail (10 mM Tris pH 6.8, 1% SDS, 10% glycerol) in the presence or absence of 4% β-mercaptoethanol and separated on either a 6.5% (non-reducing conditions) or 10% (reducing conditions) polyacrylamide gel. Non-reducing and reducing gels were transferred to immobilon-FL for 20 min in transfer buffer (25 mM Tris, 192 mM glycine) containing 20% methanol. Blots were blocked with 1% skim milk in PBS and labeled with the RS1 3R10 monoclonal antibody for 1 h and goat anti-mouse Ig conjugated to CW800 for 1hour for detection with an Odyssey Infrared Imaging System (Licor, Lincoln, NE).

3. Results

3.1. Clinical findings

A 52-year-old white man of Italian ancestry presented with a complaint of mildly reduced visual acuity and light aversion. There were no other visual complaints or relevant findings, except for history of uneventful cataract surgery one year before the exam. Family history was non-contributory. None of the patient's siblings or relatives reported any eye disease, and the proband had three healthy sons. The patient's best-corrected visual acuity was $20/40^{+2}$ in the right eye and 20/30 in the left. The anterior segment exam was unremarkable, except for presence of intra-ocular lenses in both eyes. Posterior segment examination showed a subtly dystrophic macular aspect with a sharply demarcated foveal reflex suggestive of possible previous foveal cystic appearance but no discernible schitic change (Fig. 1A). This appearance was associated with perifoveal transmission defects configuring a faint bull's eye appearance to retinal angiography (Fig. 1B) in both eyes. No macular or peripheral schitic changes were seen in either eye,

nor were any retinal breaks, tears, tractions, or demarcation lines suggestive of spontaneous resolution of a previous retinal detachment. The mid-peripheral retina was remarkable for a prominent bilateral patchy golden metallic sheen, which was much more widespread in the right eye (Fig. 1C), and fine mottling of the far-peripheral retinal pigment epithelium (RPE). Vitreous veils, more evident in the left eye than in the right, were also observed. The patient was not available for optical coherence tomography (OCT) testing.

3.2. ERG findings

Testing was remarkable for electronegative maximal ERG responses and a significant inter-ocular asymmetry (Figs. 2 and 3). In brief, in addition to the maximal ERG responses *b*-wave truncation, ERG responses in the left eye were remarkable for a mild delay of the mixed *a*-wave and a marked reduction in the amplitude of the 30 Hz flicker ERG, which was also slightly delayed. Compared to the left eye, the right eye showed: a markedly delayed and subnormal (25% smaller) rod-driven response; a more delayed and reduced (nearly 30% smaller) maximal ERG response *a*-wave and a delayed and more markedly attenuated *b*-wave (*b*/*a*-wave ratios: 0.94 in the right eye; 1.02 in the left eye; normal: >1.6); and a reduced *b*-wave (50% smaller) and slight delay of the transient light-adapted photopic ERG. Remarkably, there was no significant asymmetry in the 30 Hz flicker responses, which were both markedly attenuated and mildly delayed. Despite the lack of evidence for X-linked inheritance, the combination of these clinical and functional findings suggested the provisional diagnosis of XLRS.

3.3. Molecular genetic findings

To confirm the diagnostic impression of XLRS at the molecular level, the six exons of the *RS1* gene were sequenced as previously described (Retinoschisis Consortium, 1998), revealing a G to T change at position 336 of

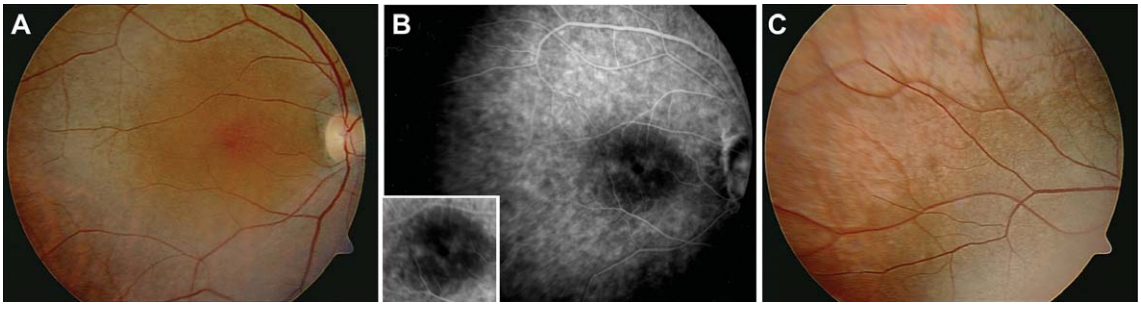

Fig. 1. Representative images of the fundus findings. (A) Posterior pole of the right eye of the proband. A dull foveal reflex and a mottled appearance of the macula were present, but no macular schisis could be observed ophthalmoscopically. (B) Mid-stage and late-stage (inset) fluorescein angiogram from the same eye, showing no change in the perifoveal hyperfluorescence, consistent with window defects due to dropout of the perifoveal retinal pigment epithelium, nearly configuring a bull's eye maculopathy. (C) View of the superotemporal quadrant of the right eye, illustrating the tapetal-like golden metallic reflex that was intense throughout the majority of the retinal mid-periphery in all quadrants of this eye. Similar but less prominent findings were present in the periphery of the left eye.

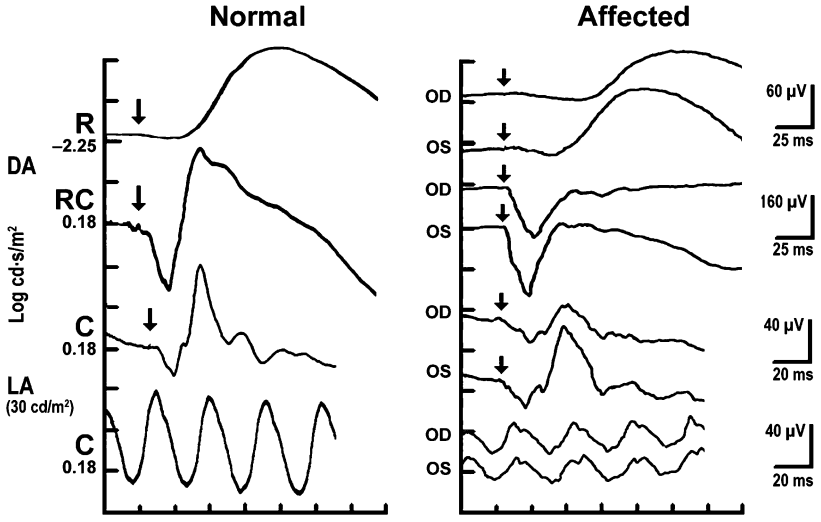

Fig. 2. ERG responses from a normal subject and from the XLRS patient harboring the W112C *RS1* mutation. Arrows identify flash onset for transient stimuli. Vertical calibration bars are for amplitudes in microvolts (μV), and horizontal calibration bars are for response timing in milliseconds (ms). DA, dark-adapted; LA, light-adapted. R, rod-driven; RC, rod/cone-driven (mixed maximal ERG response); C, cone-driven (photopic). Flash intensities are given for each stimulus condition in log cd second/meter^2. OD, right eye; OS, left eye.

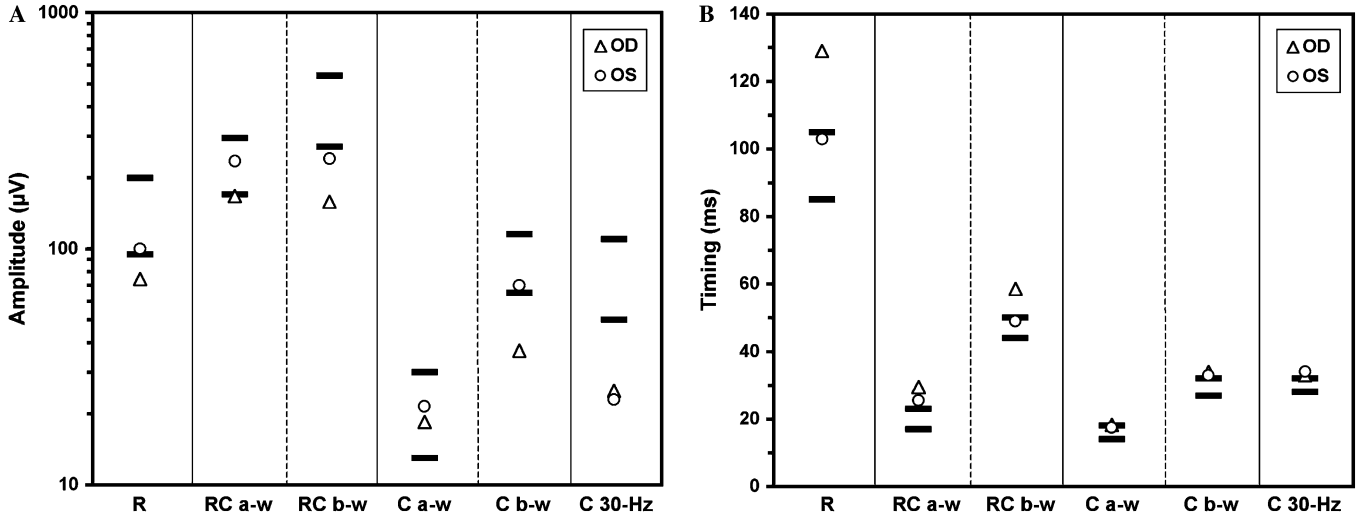

Fig. 3. Plot of ERG amplitudes (A) and timings (B). The open symbols identify the values of the patient affected with the W112C *RS1* mutation: open triangle, right eye (OD); open circle, left eye (OS). The dark horizontal bars identify the upper and the lower limit of the normal range for each parameter for this laboratory (± 2 SD). The amplitude plot, in microvolts (μV), is presented on a log scale to facilitate resolution of the data points of the affected subject. R, rod-driven; RC, rod/cone-driven (mixed maximal ERG response); C, cone-driven (photopic); a-w, *a*-wave; b-w, *b*-wave.

exon 4 (c. 336 g to t), predicting a tryptophan to cysteine amino acid substitution at codon 112 (p. Trp112Cys, or W112C). This missense mutation has been reported before in XLRS patients. The specific G → T change found in our proband has been thus far reported only in Italian patients (Retinoschisis Consortium, 1998; Simonelli et al., 2003), whereas a G → C change resulting in an identical W to C amino acid substitution has been reported also in French and Australian patients (Hewitt et al., 2005; Retinoschisis Consortium, 1998).

3.4. In vitro characterization of the W112C mutant retinoschisin protein

Previous studies have documented that most *RS1* mutations result in failure of secretion and intracellular retention of retinoschisin in the endoplasmic reticulum (ER) (Wang et al., 2002, 2006; Wu & Molday, 2003). In contrast, a few mutations result in reduced secretion, while others do not affect secretion, but prevent the assembly of retinoschisin into homo-dimers and homo-octameric complexes, two steps that are independent of one another (Wang et al., 2002, 2006; Wu & Molday, 2003; Wu et al., 2005). At the start of this study, the molecular and cellular properties W112C mutation had not been studied. Therefore, to gain insight into the mechanism underlying the distinctive clinical and functional phenotype of our proband, we expressed *RS1* with a W112C mutation in EBNA 293 cells to determine the abundance of the retinoschisin protein in the cellular and secreted fractions. Our results (Fig. 4) demonstrate that the W112C mutant is expressed at levels similar to wild-type (WT) protein and is present in the cellular fraction. However, unlike the WT protein, the W112C mutant fails to be secreted from cells either as a 24 kDa monomer or a higher molecular weight homo-octameric complex.

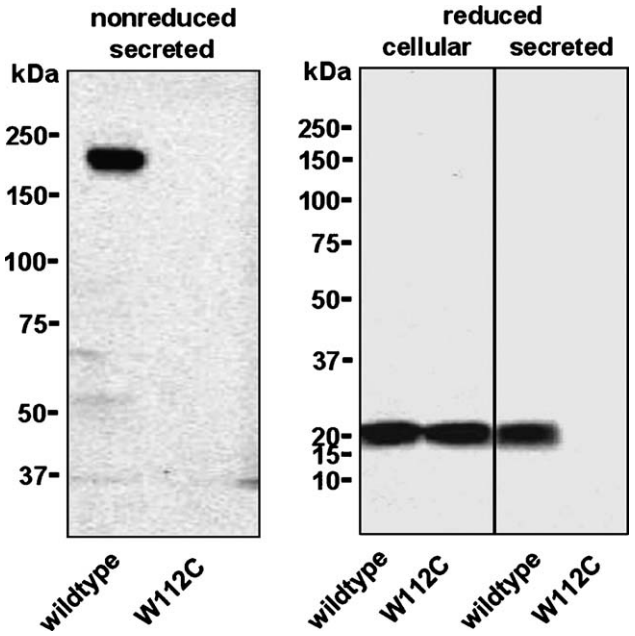

Fig. 4. Expression and secretion of wild-type (WT) and W112C mutant retinoschisin. Cells expressing WT or mutant retinoschisin were separated into the cellular (cells) and secreted fraction (medium). Retinoschisin in the secreted fraction was concentrated by immunoprecipitation. The expressed proteins were fractionated on a 6.5% or 10% SDS–polyacrylamide gel under nonreducing and reducing conditions, respectively and Western blots were labeled with the RS1 3R10 monoclonal antibody.

4. Discussion

The case of this patient highlights the importance of considering the diagnosis of XLRS whenever clinical and/or functional manifestations support such diagnosis also in the absence of clear-cut X-linked inheritance and regardless

of the age of the patient (see, for example, Nakamura, Ito, Terasaki, & Miyake, 2001), and emphasizes the benefits of molecular verification of the diagnosis, especially with regard to the counseling of the proband's three sons. The finding of the previously reported W112C mutation in this Italian patient resulting from a G → T nucleotide change thus far confirms its uniqueness to subjects of this descent.

4.1. Mild phenotype associated with the W112C mutation: Further evidence for phenotypic heterogeneity and modifiers in XLRS

Consistent with the impression that XLRS patients exhibit remarkable phenotypic variability (e.g., Inoue et al., 2000), the comparison of our findings with those of the other reported patients with the W112C mutation (Hewitt et al., 2005; Simonelli et al., 2003) confirms that there is no simple genotype-phenotype correlation in XLRS. Different from our patient, both Simonelli et al. (2003) and Hewitt et al. (2005) reported that all of their patients had macular schisis and/or atrophy of the RPE, peripheral retinoschisis in at least one eye, and often retinal detachments. It is therefore apparent that other genetic and/or epigenetic factors are likely to act as significant phenotypic modifiers in XLRS. The identification of the factors that play a determining role in mild phenotypic manifestations such as those observed in our patient may have important pathogenetic and therapeutic implications for XLRS.

4.2. The W112C mutation causes complete intracellular retention of retinoschisin

RS1 mutations can have different effects on the intraretinal fate of retinoschisin. The main effect of most mutations is defective secretion, resulting in complete intracellular retention at the level of the ER (Wang et al., 2002; Wu & Molday, 2003). Some mutations, however, cause only partially defective secretion, while others do not affect it significantly, yet they can affect the assembly of retinoschisin into homo-dimers and homo-octameric complexes, two steps that are independent of one another (Wang et al., 2006; Wu & Molday, 2003; Wu et al., 2005). Because secretion of retinoschisin is critical to its function as an extracellular protein, it was important to determine whether the secretory mechanism was altered by the W112C mutation.

A structural model of the WT discoidin domain along with the position of intramolecular disulfide bonds and the location of the conserved W112 is shown in Fig. 5. The W112 residue is buried into the discoidin domain structure with an estimated surface accessibility of only 3%. As a result, the substitution of a tryptophan with an ectopic cysteine residue (W112C) would be predicted to disrupt interactions essential for the proper folding and three-dimensional structure of its discoidin domain (Fraternali, Cavallo, & Musco, 2003). Heterologous expression of the W112C mutant in EBNA 293 cells provides support for this prediction. The W112C mutant, unlike WT retinoschisin, is

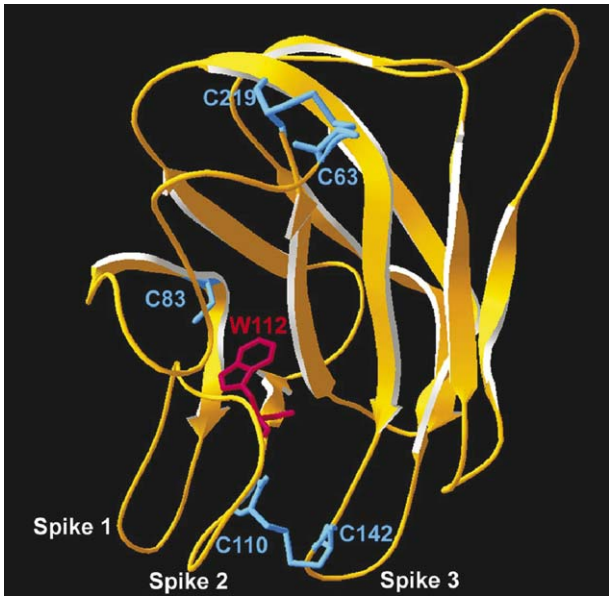

Fig. 5. A ribbon model for the discoidin domain of retinoschisin showing the location of the W112 residue. The discoidin domain of RS1 is shown to have a barrel-like structure consisting of eight beta strands with spikes projecting from one end of the structure. The location of W112 (red) and the C63-C219 and C110-C142 intramolecular disulfide bonds (blue) is shown. The W112 residue is buried inside the discoidin domain structure, where it contributes to the folding and structure of the protein. The model was generated as described by Wu and Molday (2003).

retained in the ER by the quality control system of the cell, which prevents secretion of misfolded proteins. Moreover, an additional cysteine at position 112 can result in the formation of aberrant intermolecular disulfide bonds resulting in protein aggregation within the lumen of the ER (Wu & Molday, 2003). During the course of our studies, Wang et al. (Wang et al., 2006) extended their in vitro studies of disease-linked retinoschisin mutants. In this study, they reported that the W112C mutant fails to be secreted from COS-7 cells transfected with this mutant, a result that is in agreement with our studies reported here using EBNA 293 cells.

4.3. ERG abnormalities: a pattern consistent with coexistence of ON- and OFF-pathway defects

A defect in photoreceptor-to-bipolar cell synapses or in bipolar cells themselves likely explains the ERG abnormalities observed in our patient, a finding that fits well with the expression pattern of retinoschisin (Molday et al., 2001; Reid et al., 2003; Reid & Farber, 2005; Takada et al., 2004; Wu & Molday, 2003) and the observed disruption of the photoreceptor-to-bipolar synapse observed in *Rs1h* knockout mice (Weber et al., 2002). Abnormalities of both ON and OFF ERG responses have been reported in XLRS (Alexander, Barnes, & Fishman, 2001a; Alexander, Fishman, Barnes, & Grover, 2001b; Khan, Jamison, Kemp, & Sieving, 2001; Shinoda et al., 2001). Based on the current understanding of the origin of full-field ERG components

(Bush & Sieving, 1994; Khan et al., 2005; Kondo & Sieving, 2001, 2002; Sieving, Murayama, & Naarendorp, 1994), the abnormalities observed in the dark-adapted transient ERG responses of our patient are best explained by a selective or prevailing dysfunction of depolarizing ON-bipolar cells, more severe in the right eye. This appears to be case also for the transient photopic ERG of this patient, which resembled very closely that obtained in monkeys following ON-pathway blockade (Bush & Sieving, 1994). However, the bilateral and symmetric marked reduction in the amplitude of the flicker response is not adequately explained by an ON-pathway defect.

ERG studies by Kondo and Sieving (Kondo & Sieving, 2002) in primates have shown that the clinical 30 Hz light-adapted strobe flash-evoked photopic ERG response would not be expected to be substantially reduced in amplitude as a result of a selective ON-pathway block. By analogy (Kondo & Sieving, 2002), we propose that, at least in response to the stimuli of the type, frequency and intensity used here, the 30 Hz flicker symmetrically reduced amplitude is best explained by the coexistence of an OFF-pathway dysfunction, likely present in both eyes to an approximately identical extent. This interpretation of the flicker ERG results is consistent with the notion that the flicker ERG probes the photopic system differently than the transient cone ERG and is in line also with the studies conducted by Khan et al. on other XLRS patients (Khan et al., 2001).

It remains unclear why would the retinal sheen correlate only with the degree of ON-pathway compromise and why would an asymmetry in retinal dysfunction exist only for the ON- and not the OFF-pathway. A possible answer may lie in the "push-pull" model with which Sieving et al. (Sieving et al., 1994) characterized the interaction between second-order neurons of the ON- and OFF-photopic pathways and their effects on the generation of the photopic ERG. It must be noted, though, that additional complexities of the cone pathways have been recently revealed (Khan et al., 2005). Therefore, yet unknown aspects of the regulation and responsiveness of retinal microcircuitry may also account for this observation.

4.4. The tapetal-like metallic reflex in XLRS: a sub-clinical disease expression resulting from intracellular retention of retinoschisin?

The clinical and functional significance of the tapetal-like metallic reflex in XLRS is not fully understood. The tapetal-like sheen observed in our patient was not reported in any of the XLRS patients described by either Simonelli et al. (Simonelli et al., 2003) Hewitt et al. (Hewitt et al., 2005), or in the first report of the W112C mutation (Retinoschisis Consortium, 1998). The presence of a tapetal-like reflex has instead been noted in other XLRS patients with verified *RS1* mutations (see online Table for a complete list) (Eksandh et al., 2000; Inoue et al., 2000; Mendoza-Londono et al., 1999; Sato, Oshika, Kaji, & Nose, 2003; Shinoda, Ishida, Oguchi, & Mashima, 2000; Shinoda et al., 2001; Tanimoto et al., 2002; Tuvdendorj, Isashiki, Ohba, Sonoda, & Izumo, 2002), but its correlation with ERG findings, if any, has neither been reported nor investigated.

Tapetal-like retinal reflexes characterize also other retinal diseases (reviewed by (Cideciyan & Jacobson, 1994)). The origin of these reflexes has been studied in female carriers of X-linked retinitis pigmentosa, showing that they likely originate from photoreceptors (Cideciyan & Jacobson, 1994; Berendschot, DeLint, & van Norren, 1996). Retinoschisin has been localized to retinal photoreceptors in several independent studies (Molday et al., 2001; Reid et al., 1999; Reid & Farber, 2005; Takada et al., 2004; Wang et al., 2002; Wu & Molday, 2003) and *RS1* mutations are predicted to result most often in defective secretion of retinoschisin (Wang et al., 2002; Wu & Molday, 2003). We have provided evidence that also the W112C mutation results in complete intracellular retention of the mutant protein. Although caution remains always warranted in assuming that any in vitro data accounted in full for the entire range of in vivo pathological effects of any mutation, this behavior would predict a severe disruption of retinal micro- and macro-anatomy, as observed in the family reported by Simonelli et al. (2003). This was clearly not the case in our subject.

It is therefore conceivable that the mitigating genetic and/or epigenetic modifiers that account for the overall mild disease manifestations seen in our patient also allowed for the retention of retinoschisin in photoreceptor cells to result in the observed tapetal-like reflex without leading to overt schitic changes. Its proportionality to the severity of ERG changes supports the notion that the sheen likely represents a sub-clinical phenotypic expression of XLRS with a discernible functional counterpart appreciable at the ERG level, such that a greater degree of intracellular retention in photoreceptors would result in a larger adverse effect on post-receptoral ERG responses.

Although it has been shown that retinoschisin may undergo transcytotic transport through Müller cells (Reid & Farber, 2005), the complete lack of secretion experienced by the W112C mutant protein argues against any direct involvement of this putative mechanism in the biogenesis of the sheen, but does not conclusively rule out the postulated role of excess extracellular K^+ ions suggested by de Jong et al (de Jong et al., 1991). It remains to be determined whether the tapetal-like metallic sheen of XLRS is directly due to photoreceptor intracellular retention of retinoschisin, to mislocalization of the mutant protein at the photoreceptor-to-bipolar cell synapse or, in fact, to some entirely different mechanism linked to lack of extracellular release of retinoschisin.

5. Conclusions

In summary, we have reported an unusually late-onset and mild retinal phenotype associated with the W112C mutation of the *RS1* gene. This unique phenotype had not

been previously reported in association with this mutation. Moreover, we demonstrated that the mutant W112C protein fails to be secreted from EBNA 293 cells. Continued functional characterization of clinical XLRS phenotypes, investigation of the effects of specific mutations on the intraretinal fate of the mutated protein, and identification of retinoschisin-interacting proteins in the retina will hopefully shed light on the clinical and functional phenotypic variability of XLRS and reveal in full the pathophysiology of this protean disorder. An answer to these prevailing questions may be facilitated by the recent identification of an ENU-mutagenized mouse line harboring a mutation in the *Rs1h* gene with retinal histopathologic features closely resembling those reported in human XLRS retinas (Jablonski et al., 2005). It will therefore soon become possible to investigate the in vivo fate of persistent yet defective retinoschisin production and its effect on retinal cytoarchitecture and function in an animal model resembling even more closely the human scenarios.

Acknowledgments

The authors gratefully acknowledge support from: Grant-in-Aid GA03048, Fight for Sight, New York, NY (A.I.); Research to Prevent Blindness, Inc., New York, NY (unrestricted grants to UTHSC Department of Ophthalmology and U.M. Department of Ophthalmology and Visual Sciences; Career Development Award to A.I.; and Sybil Harrington Special Scholar Award to R.A., and a Arthur and June Wilms Fellowship to F.M.D.); Grants no. EY02422 (R.S.M.), EY13198 (R.A.), EY07003 and EY07060 (core grants, UM Department of Ophthalmology and Visual Sciences) and EY13080 (core grant, UTHSC Department of Ophthalmology) National Eye Institute, NIH, Bethesda, MD; and Foundation Fighting Blindness, Owing Mills, MD (R.A.). We also thank Dr. Paul A. Sieving, M.D., Ph.D., National Eye Institute, NIH, Bethesda, MD (USA) for his insightful comments and suggestions in the early stages of this investigation.

Appendix A. Supplementary data

Supplementary data associated with this article can be found, in the online version, at doi:10.1016/j.visres.2006.06.011.

References

Alexander, K. R., Barnes, C. S., & Fishman, G. A. (2001a). High-frequency attenuation of the cone erg and on-response deficits in x-linked retinoschisis. *Investigative Ophthalmology & Visual Science, 42*, 2094–2101.

Alexander, K. R., Fishman, G. A., Barnes, C. S., & Grover, S. (2001b). On-response deficit in the electroretinogram of the cone system in x-linked retinoschisis. *Investigative Ophthalmology & Visual Science, 42*, 453–459.

Berendschot, T. T. J. M., DeLint, P. J., & van Norren, D. (1996). Origin of tapetal-like reflexes in carriers of x-linked retinitis pigmentosa. *Investigative Ophthalmology & Visual Science, 37*, 2716–2723.

Bush, R. A., & Sieving, P. A. (1994). A proximal retinal component in the primate photopic erg a-wave. *Investigative Ophthalmology & Visual Science, 35*, 635–645.

Cideciyan, A., & Jacobson, S. (1994). Image analysis of the tapetal-like reflex in carriers of x-linked retinitis pigmentosa. *Investigative Ophthalmology & Visual Science, 35*, 3812–3824.

de Jong, P., Zrenner, E., van Meel, G., Keunen, J., & van Norren, D. (1991). Mizuo phenomenon in x-linked retinoschisis. Pathogenesis of the mizuo phenomenon. *Archives of Ophthalmology, 109*, 1104–1108.

Eksandh, L. C., Ponjavic, V., Ayyagari, R., Bingham, E. L., Hiriyanna, K. T., Andreasson, S., et al. (2000). Phenotypic expression of juvenile x-linked retinoschisis in swedish families with different mutations in the xlrs1 gene. *Archives of Ophthalmology, 118*, 1098–1104.

Falcone, P. M., & Brockhurst, R. J. (1993). X-chromosome-linked juvenile retinoschisis: Clinical aspects and genetics. *International Ophthalmology Clinics, 33*, 193–202.

Fraternali, F., Cavallo, L., & Musco, G. (2003). Effects of pathological mutations on the stability of a conserved amino acid triad in retinoschisin. *FEBS Letters, 544*, 21–26.

George, N., Yates, J., & Moore, A. (1995). X linked retinoschisis. *British Journal of Ophthalmology, 79*, 697–702.

George, N. D. L., Yates, J. R. W., & Moore, A. T. (1996). Clinical features in affected males with x-linked retinoschisis. *Archives of Ophthalmology, 114*, 274–280.

Hewitt, A. W., FitzGerald, L. M., Scotter, L. W., Mulhall, L. E., McKay, J. D., & Mackey, D. A. (2005). Genotypic and phenotypic spectrum of x-linked retinoschisis in australia. *Clinical & Experimental Ophthalmology, 33*, 233–239.

Inoue, Y., Yamamoto, S., Okada, M., Tsujikawa, M., Inoue, T., Okada, A. A., et al. (2000). X-linked retinoschisis with point mutations in the xlrs1 gene. *Archives of Ophthalmology, 118*, 93–96.

Jablonski, M. M., Dalke, C., Wang, X., Lu, L., Manly, K. F., Pretsch, W., et al. (2005). An enu-induced mutation in rs1h causes disruption of retinal structure and function. *Molecular Vision, 11*, 569–581.

Kellner, U., Brummer, S., Foerster, M. H., & Wessing, A. (1990). X-linked congenital retinoschisis. *Graefe's Archives for Clinical and Experimental Ophthalmology, 228*, 432–437.

Khan, N. W., Jamison, J. A., Kemp, J. A., & Sieving, P. A. (2001). Analysis of photoreceptor function and inner retinal activity in juvenile x-linked retinoschisis. *Vision Research, 41*, 3931–3942.

Khan, N. W., Kondo, M., Hiriyanna, K. T., Jamison, J. A., Bush, R. A., & Sieving, P. A. (2005). Primate retinal signaling pathways: Suppressing on-pathway activity in monkey with glutamate analogs mimics human genetic csnb1-nyx night blindness. *Journal of Neurophysiology, 93*, 481–492.

Koenekoop, R. K., Fishman, G. A., Iannaccone, A., Ciccarelli, M. L., Ezzeldin, H., Baldi, A., et al. (2002). Electroretinographic and psychophysical abnormalities in parents of leber congenital amaurosis patients. *Archives of Ophthalmology, 120*, 1325–1330.

Kondo, M., & Sieving, P. A. (2001). Primate photopic sine-wave flicker erg: Vector modeling analysis of component origins using glutamate analogs. *Investigative Ophthalmology & Visual Science, 42*, 305–312.

Kondo, M., & Sieving, P. A. (2002). Post-photoreceptoral activity dominates primate photopic 32-hz erg for sine-, square-, and pulsed stimuli. *Investigative Ophthalmology & Visual Science, 43*, 2500–2507.

Mendoza-Londono, R., Hiriyanna, K. T., Bingham, E. L., Rodriguez, F., Shastry, B. S., Rodriguez, A., et al. (1999). A colombian family with x-linked juvenile retinoschisis with three affected females finding of a frameshift mutation. *Ophthalmic Genetics, 20*, 37–43.

Molday, L. L., Cook, N. J., Kaupp, U. B., & Molday, R. S. (1990). The cgmp-gated cation channel of bovine rod photoreceptor cells is associated with a 240-kda protein exhibiting immunochemical cross-reactivity with spectrin. *The Journal of Biological Chemistry, 265*, 18690–18695.

Molday, L. L., Hicks, D., Sauer, C. G., Weber, B. H. F., & Molday, R. S. (2001). Expression of x-linked retinoschisis protein rs1 in photoreceptor and bipolar cells. *Investigative Ophthalmology & Visual Science, 42*, 816–825.

Nakamura, M., Ito, S., Terasaki, H., & Miyake, Y. (2001). Japanese x-linked juvenile retinoschisis: Conflict of phenotype and genotype with novel mutations in the xlrs1 gene. *Archives of Ophthalmology, 119*, 1553–1554.

Pannarale, M. R., Grammatico, B., Iannaccone, A., Forte, R., De Bernardo, C., Flagiello, L., et al. (1996). Autosomal dominant retinitis pigmentosa associated with an arg-135-trp point mutation of the rhodopsin gene: Clinical features and longitudinal observations. *Ophthalmology, 103*, 1443–1452.

Reid, S. N., Akhmedov, N. B., Piriev, N. I., Kozak, C. A., Dancinger, M., & Farber, D. B. (1999). The mouse x-linked retinoschisis cdna: Expression in photoreceptors. *Gene, 227*, 257–266.

Reid, S. N., Yamashita, C., & Farber, D. B. (2003). Retinoschisin, a photoreceptor-secreted protein, and its interaction with bipolar and muller cells. *The Journal of Neuroscience, 23*, 6030–6040.

Reid, S. N., & Farber, D. B. (2005). Glial transcytosis of a photoreceptor-secreted signaling protein, retinoschisin. *Glia, 49*, 397–406.

Retinoschisis Consortium (1998). Functional implications of the spectrum of mutations found in 234 cases with x-linked juvenile retinoschisis (xlrs). *Human Molecular Genetics, 7*, 1185–1192.

Sato, M., Oshika, T., Kaji, Y., & Nose, H. (2003). Three novel mutations in the x-linked juvenile retinoschisis (xlrs1) gene in 6 japanese patients, 1 of whom had turner's syndrome. *Ophthalmic Research, 35*, 295–300.

Sauer, C. G., Gehrig, A., Warnecke-Wittstock, R., Marquardt, A., Ewing, C. C., Gibson, A., et al. (1997). Positional cloning of the gene associated with x-linked juvenile retinoschisis. *Nature Genetics, 17*, 164–170.

Shinoda, K., Ishida, S., Oguchi, Y., & Mashima, Y. (2000). Clinical characteristics of 14 japanese patients with x-linked juvenile retinoschisis associated with xlrs1 mutation. *Ophthalmic Genetics, 21*, 171–180.

Shinoda, K., Ohde, H., Mashima, Y., Inoue, R., Ishida, S., Inoue, M., et al. (2001). On- and off-responses of the photopic electroretinograms in x-linked juvenile retinoschisis. *American Journal of Ophthalmology, 131*, 489–494.

Sieving, P. A., Murayama, K., & Naarendorp, F. (1994). Push-pull model of the primate photopic electroretinogram: A role for hyperpolarizing neurons in shaping the b-wave. *Visual Neuroscience, 11*, 519–532.

Simonelli, F., Cennamo, G., Ziviello, C., Testa, F., de Crecchio, G., Nesti, A., et al. (2003). Clinical features of x linked juvenile retinoschisis associated with new mutations in the xlrs1 gene in italian families. *The British Journal of Ophthalmology, 87*, 1130–1134.

Takada, Y., Fariss, R. N., Tanikawa, A., Zeng, Y., Carper, D., Bush, R., et al. (2004). A retinal neuronal developmental wave of retinoschisin expression begins in ganglion cells during layer formation. *Investigative Ophthalmology & Visual Science, 45*, 3302–3312.

Tanimoto, N., Usui, T., Takagi, M., Hasegawa, S., Abe, H., Sekiya, K., et al. (2002). Electroretinographic findings in three family members with x-linked juvenile retinoschisis associated with a novel pro192thr mutation of the xlrs1 gene. *Japanese Journal of Ophthalmology, 46*, 568–576.

Tuvdendorj, D., Isashiki, Y., Ohba, N., Sonoda, S., & Izumo, S. (2002). Two japanese patients with mutations in the xlrs1 gene. *Retina, 22*, 354–357.

Wang, T., Waters, C. T., Rothman, A. M., Jakins, T. J., Romisch, K., & Trump, D. (2002). Intracellular retention of mutant retinoschisin is the pathological mechanism underlying x-linked retinoschisis. *Human Molecular Genetics, 11*, 3097–3105.

Wang, T., Zhou, A., Waters, C. T., O'Connor, E., Read, R. J., & Trump, D. (2006). Molecular pathology of x linked retinoschisis: Mutations interfere with retinoschisin secretion and oligomerisation. *The British Journal of Ophthalmology, 90*, 81–86.

Weber, B. H., Schrewe, H., Molday, L. L., Gehrig, A., White, K. L., Seeliger, M. W., et al. (2002). Inactivation of the murine x-linked juvenile retinoschisis gene, rs1h, suggests a role of retinoschisin in retinal cell layer organization and synaptic structure. *Proceedings of the National Academy of Sciences of the United States of America, 99*, 6222–6227.

Wu, W. W., & Molday, R. S. (2003). Defective discoidin domain structure, subunit assembly, and endoplasmic reticulum processing of retinoschisin are primary mechanisms responsible for x-linked retinoschisis. *The Journal of Biological Chemistry, 278*, 28139–28146.

Wu, W. W., Wong, J. P., Kast, J., & Molday, R. S. (2005). Rs1, a discoidin domain containing retinal cell adhesion protein associated with x-linked retinoshcisis, exists as a novel disulfide-linked octamer. *The Journal of Biological Chemistry, 280*, 10721–10730.